



# 1 **Chemical ozone loss and chlorine activation in the Antarctic winters** 2 **2013–2020**

3  
4 Raina Roy<sup>1,2</sup>, Pankaj Kumar<sup>1</sup>, Jayanarayanan Kuttippurath<sup>1</sup>, Franck Lefevre<sup>3</sup>

5  
6 <sup>1</sup>*CORAL, Indian Institute of Technology Kharagpur, Kharagpur–721302, India.*

7 <sup>2</sup>*Department of Physical Oceanography, Cochin University of Science and Technology, Kochi, India.*

8 <sup>3</sup>*LATMOS/IPSL, Sorbonne Université, UVSQ, CNRS, Paris, France*

9  
10 *Correspondence to:* Raina Roy (rainaroy2105@gmail.com)

## 11 **ABSTRACT**

12  
13 Since its discovery in 1985, the formation of ozone holes in the Antarctic and the resulting ultra-violet (UV)  
14 radiation reaching the planet's surface has been a source of major concern. The annual formation of ozone hole in  
15 the austral springs has regional and global climate implications. Ozone depletion episodes can change precipitation,  
16 temperature, and atmospheric circulation patterns, affecting the surface climate primarily in the southern  
17 hemisphere (SH). Therefore, the study of ozone loss variability is important to assess its consequential effects on  
18 the climate and public health. Our study examines and quantifies the ozone loss and its cycle for the past 8 years  
19 in the Antarctic using satellite measurements (Microwave Limb Sounder on Aura). We observe the highest ozone  
20 loss (3.8–4.0 ppmv) in spring 2020 followed by 2016. The high chlorine activation (2.3 ppbv), stable polar vortex  
21 and extensive areas of polar stratospheric clouds (PSCs) (12.6 Million Km<sup>2</sup>) favored the large ozone loss in 2000.  
22 The spring of 2019 also witnessed a moderately high ozone loss, although the year was marked by a rare minor  
23 warming in mid-September. Relatively smaller ozone loss (2.4–2.5 ppmv) was present in 2017 and 2015. It was  
24 mainly due to reduced chlorine activation and relatively higher temperature in these winters. Additionally, the  
25 chlorine activation in 2015 (1.95 ppbv) was the lowest and the wave forcing from the lower latitudes was very high  
26 in 2017 (up to -60 Kms<sup>-1</sup>). The analysis shows significant interannual variability in the Antarctic ozone as for the  
27 immediate previous decade. The study helps to understand the role of the dynamics and chemistry in the inter-  
28 annual variability of ozone depletion for the years.

29  
30 **Keywords:** Antarctica; Ozone loss estimates; Polar Vortex; climate Change; Model simulations

31 **Short title:** Antarctic ozone loss in 2013–2020



## 32 INTRODUCTION

33

34 An important event in the Antarctic stratosphere during the austral spring that has caught global attention ever since  
35 its discovery in the 1980s is the Antarctic ozone hole (Farman et al., 1985). The chlorine free-radicals released  
36 from the chlorofluorocarbons (CFCs) and other ozone-depleting substances (ODSs) activate the catalytic cycles  
37 that led to severe ozone loss (e.g. Stolarski and Cicerone, 1974; Rowland et al., 1976). The extreme cold conditions  
38 that prevail in the poles facilitate the formation of Polar Stratospheric Clouds (PSCs), which serve as the activation  
39 surface for the ODSs. Apart from these, the relatively stable Antarctic polar vortex also contributes significantly to  
40 the formation of ozone holes annually (Solomon et al., 2014). Since the discovery of ODSs in the 1970s from  
41 anthropogenic activities, the ozone loss continued to rise and reached its worst phase in the late 1980s and early  
42 1990s (WMO, 2014; Kuttippurath et al., 2015). The growth in the ODSs was curtailed after the enactment of the  
43 Montreal Protocol in 1987. Ratifying of the environmental treaty led to a stabilisation of the loss from the late  
44 1990s to the early 2000s in the Antarctic. Despite this, there was no significant increase in total column ozone  
45 during those times (e.g. Weatherhead et al., 2000; WMO, 2007; Angell et al., 2009). Beyond 2000, significant  
46 recovery trends in the ozone were presented with evidence from both ground or satellite observations (e.g. Yang et  
47 al., 2008; Salby et al., 2011; Solomon et al., 2016; Chipperfield et al., 2017; Kuttippurath and Nair, 2017; de Laat  
48 et al., 2017; Pazmiño et al., 2018; Wespes et al., 2019). A reduction in the saturation of ozone loss over the period  
49 2001–2017 was also observed in the Antarctic and thus confirming the positive ozone trends in the region  
50 (Kuttippurath et al., 2018).

51 The rate of ozone loss in the Antarctic is ascertained by a combination of both polar vortex dynamics and chemistry  
52 of the winters. Analyses performed by Nedoluha et al. (2016); Strahan et al. (2014); and Strahan et al. (2018)  
53 confirmed the importance of chlorine concentration for the formation of ozone holes. They observed a significant  
54 reduction in the amount of chlorine free radicals in the twenty-first century and thus, a consistent increase in the  
55 corresponding ozone concentration. On the contrary, the longer lifetimes of ODSs (SPARC, 2016), the non-  
56 compliance to the protocol and the recent emissions of the ODSs such as CFC-11, brominated ODSs and several  
57 other short-lived ODSs (e.g. Maione et al., 2014; Rigby et al., 2017; Montzka et al., 2018; Dhomse et al., 2019),  
58 and the increasing emissions of nitrogen oxides (e.g. Butler et al., 2016; Maliniemi et al., 2021) all of which  
59 subsequently decelerated the recovery rate of ozone. An evident manifestation of the influence of dynamic  
60 variability in the Antarctic polar vortex is found in the years such as 2000, 2002 and 2004 (Langematz and Kunze,  
61 2006). Thus, the polar vortex variability is an important factor that controls the rate of ozone depletion (e.g.



62 Stolarski et al., 2006; Zhang et al., 2017). Therefore, a combined action of vortex dynamics and stratospheric  
63 chemistry can only lead to significant changes in the Antarctic ozone concentration. The study of annual ozone loss  
64 is important as the changes in ozone directly and indirectly affect the climate of southern hemisphere (SH),  
65 precipitation patterns, and the circulation in austral summer (e.g. Polvani et al., 2011; Bandoro et al., 2014; Damiani  
66 et al., 2020)

67 Here, we present the long-term analysis of ozone loss for the winters 2013–2020 considering the chemical and  
68 dynamical characteristics of the periods prior to and of peak ozone loss. Although a few of the years have been  
69 studied individually, the long-term analysis helps in better understanding the evolution of the springs/winters  
70 (e.g. WMO, 2015; Krummel et al., 2016; Wargan et al., 2020; Klekociuk et al., 2021). The dynamics of these  
71 winters are studied using different meteorological parameters. The study offers a high-resolution analysis of the  
72 interannual variability of ozone loss at various altitudes using the data obtained from the AURA microwave Limb  
73 Sounder (MLS) (Froidevaux et al., 2008; Santee et al., 2008b). The ozone loss is calculated using the passive tracer  
74 simulated by the REPROBUS (Reactive Processes Ruling the Ozone Budget in the Stratosphere) chemical transport  
75 model (CTM) (Lefèvre et al., 1994). Therefore, we use a single data set and the same method to estimate ozone  
76 loss for all eight years to assess the interannual variability, which would make the comparisons among the winters  
77 and assessment of polar winters meaningful and coherent.

## 78 **DATA AND METHODS**

79

80 We have analysed the meteorology of the winters from 2013 to 2020 using the Modern-Era Retrospective analysis  
81 for Research and Applications (MERRA-2) data (Gelaro et al., 2017). The MERRA 2 data are available for 42  
82 pressure levels with a spatial resolution of  $0.5^\circ \times 0.625^\circ$ . The nature of austral springs is studied by the examination  
83 of four parameters such as the polar cap temperature, zonally averaged from  $60^\circ$  to  $90^\circ\text{S}$  at 100 hPa, the minimum  
84 polar cap temperature at 10 hPa, the area of polar stratospheric clouds at 460 K, and the mean heat flux averaged  
85 from  $45^\circ$  to  $75^\circ\text{S}$ . Besides, the MERRA 2 dataset is also employed to analyse the vertical evolution of temperature  
86 averaged from  $60^\circ$  to  $90^\circ\text{S}$ .

87 We calculate the ozone loss using the REPROBUS model simulations. The model simulates a passive tracer  
88 identical to ozone to estimate the loss in each year. It is a three-dimensional model driven by the European Centre  
89 for Medium-Range Weather Forecasts (ECMWF) operational analyses. The analysis is performed over the altitude  
90 range 1000 to 0.01 hPa (130 levels) (Dee et al., 2011). In the model, the advection is performed by the winds on



91 the hybrid sigma pressure coordinates and the trace gases are advected by a semi-lagrangian technique (Williamson  
92 and Rasch, 1989). For our study, the passive tracer identical to the ozone was initialized on July 1 of each year and  
93 continued until the end of November. Then the loss is computed by subtracting the measured ozone from the  
94 modelled passive tracer. The loss in each day is estimated inside the polar vortex as it is more prevalent there and  
95 thus, the polar vortex edge is calculated using the equivalent latitude (Nash et al., 1996; Müller et al., 2005).

96 The ozone and the chlorine monoxide data are taken from the AURA microwave limb sounder (MLS). The MLS  
97 data of version 4.2 is used. The data have a vertical resolution of 2–3 km, a vertical range of 261–0.02 hPa and an  
98 accuracy of 0.1–0.4 ppmv. Along with this, the ClO measurements are obtained at 640 GHz and are about 3–3.5  
99 km over 147–1 hPa, and the accuracy of measurements is about 0.2–0.4 ppbv. These measurements have a latitude-  
100 dependent bias of around 0.2–0.4 ppbv, depending on vertical height (Livesay et al., 2013).

## 101 **RESULTS AND DISCUSSION**

102

### 103 **Meteorology of the winters**

104

105 Figure 1 shows the meteorology of the winters as illustrated, with the polar cap temperature (60–90°S) at 100 hPa,  
106 minimum temperature averaged at 50°–90° S at 100 hPa, PSC area (460 K) and mean heat flux from 45° to 75°S  
107 at 100 hPa. The first panel shows the mean temperature (60°–90°S) at 100 hPa, the different coloured lines represent  
108 individual years. The lowest temperature for all the years is observed during August. The temperature begins to  
109 decrease since the beginning of winter (June) and reaches the lowest in August. It is observed from Fig. 1 that all  
110 the years have a temperature in the order of 195–208 K during this period. In the years 2013, 2014, 2015 and 2020  
111 the temperature reduces below 195 K (PSC formation threshold) for a short while in August. However, the  
112 temperature in 2019 shows a sudden rise from late August (202 K) to mid-September (218 K), indicative of the  
113 occurrence of a Sudden Stratospheric Warming (SSW) event. This event has been reported in many of the previous  
114 studies and has been described as a minor Warming (mW) (e.g. Shen et al., 2020a,b; Yamazaki et al., 2020). The  
115 temperature in August 2017 is also seen to be higher than the other years but lower than that in 2019. There is a  
116 visible rise in temperature in the beginning of austral spring. However, temperatures persist below 195 K during  
117 early September in 2015. The lowest temperature range during the spring-winter is present in 2015. The  
118 temperatures in 2020 also follow this range closely, as depicted in Fig 1.



119 Second panel of Fig 1 shows the minimum temperature during the day averaged in the latitudes surrounding the  
120 polar cap. The minimum temperature for all the winters is found to be lower than the PSC formation threshold.  
121 This continues for the early spring for all the years except 2019 and the minimum value rises soon after and is  
122 higher than 195 K in late spring. The minimum temperature reached their lowest during the day for most days  
123 during the spring and winter of 2015, 2018 and 2020. Thus, ideal conditions for the formation of PSCs are found  
124 for the majority of winter and spring in all 8 years. Therefore, the PSC area grows since the beginning of austral  
125 winter and is observed to be the highest in August (up to 28 million Km<sup>2</sup>). Corresponding to the periods of longest  
126 minimum temperature, the PSCs are estimated to persist until early November in 2015, 2018 and 2020, but are  
127 short-lived in 2017 and 2019. As the mean temperature peaks in early to mid-September in 2019, the PSC area  
128 drops and diminishes by late September. They dissipated by mid-October in 2017.

129 A major factor affecting the strength of the polar vortex is the tropospheric forcing. The strength of these forcings  
130 is highly reduced in the Antarctic except for a few winters. In the study of Zuev et al. (2019), the strengthening of  
131 the Antarctic polar vortex in winter and spring is due to the seasonal temperature variations in the subtropical lower  
132 stratosphere. The last panel of Fig 1 shows the tropospheric forcing for the years. The heat flux forcings averaged  
133 between the adjacent mid-latitude and higher latitudes is found to be directed southwards particularly in late winter  
134 and early spring. The years 2019 and 2017 are characterised by very wave forcings, as shown by the flux (from -  
135 40 to -50 Kms<sup>-1</sup>) in the figure. The study conducted by Klekociuk et al. (2020) reported that the easterly phase of  
136 QBO in 2017 also favoured the influence of enhanced wave activity on the polar vortex. The studies of Milinevsky  
137 et al. (2019) and Evtushevsky et al. (2020) also imply similar results about both winters. The zonal average of heat  
138 flux stays between -30 Kms<sup>-1</sup> and 10 Kms<sup>-1</sup> for much of the winter and the flux increases as the spring approaches.  
139 The magnitude of these forcings is limited for the years 2015 and 2020.

#### 140 **Temporal evolution of temperature with altitude**

141 Figure 2 represents the temporal evolution of zonal mean (60°–90°S) temperature profile in the Antarctic for the  
142 years 2013–2020. The coloured contours show the growth of temperature across the seasons. The white contour  
143 lines represent 188, 195 and 210 K. The zonal winds (westerlies) are overlaid in the figure using the black contour  
144 lines and the easterlies are shown in red. The higher temperature contours descend to the lower stratosphere towards  
145 the end of austral spring. From the analysis, we observe that the descent to the lower stratosphere is maximum in  
146 2019 during mid-September as a consequence of the minor warming. The temperature contours in the range 250–  
147 265 K extend to slightly below 10 hPa. We also notice a slight reduction in the speed of westerlies during the



148 period. The zonal mean temperature contours reveal that temperatures below 195 K are found in the lower  
149 stratosphere (100–70 hPa) until mid-October in 2015 and 2020. This implies that the temperature conditions during  
150 these years are the most ideal for the highest ozone loss. Similarly, the area covered by 195 K is also moderately  
151 high in 2013, 2014, 2016 and 2018. However, this is lowest in 2019 and is minimal in 2017. The appearance of  
152 easterlies below the 10 hPa altitude is late in 2015 (late November) whereas in 2019 and 2017 the easterlies appear  
153 as early as late October. Thus, the vortex lasted the longest in 2015.

### 154 **Temporal evolution of ozone**

155  
156 Figure 3 shows the temporal evolution of ozone (in ppmv) from MLS data for the period 2013–2020. It is observed  
157 from previous studies that the ozone loss is maximum in the lower stratosphere in all years (Solomon et al., 1990).  
158 The ozone concentration reduces in the lower altitudes every year as time progresses (mainly in spring), as  
159 illustrated in Fig 3. Opposed to this, the concentration of ozone in the upper stratosphere increases as time evolves.  
160 The ozone concentration in the years 2013, 2014, 2015, 2016, 2018 and 2020 in the lower altitudes (400–600 K) is  
161 around 0–3 ppmv. Unlike in the cold winters/springs, the concentration of ozone is slightly higher (1.5–2.5 ppmv)  
162 in the same altitude range in 2019. Similarly, in 2017, the ozone concentration in the lower stratosphere is higher  
163 than the previous cold years owing to the higher temperature present in the stratosphere. The lowest ozone  
164 concentration for the altitude range 400–475 K is observed during the years 2018 and 2020. The 0.5 ppmv contour  
165 extends to a level of 475–500 K in both years.

### 167 **Chlorine activation and ozone loss in 2013–2019.**

168  
169 Figure 4 presents the temporal evolution of ClO (right) and ozone loss (left) at different altitudes during the period  
170 of study. The ozone loss is highest in the altitude range 400–550 K or in the lower stratosphere for all years and is  
171 observed in September and October. The loss is less than 1.4 ppmv in the upper stratosphere in all years. The ozone  
172 loss in 2014 and 2015 are almost similar, at about 2.6–3.0 ppmv in the peak ozone loss altitude during September  
173 and October. The ozone loss in 2013 reaches up to 3.2 ppmv in mid-October and is higher than that in 2014 and  
174 2015 (Vargin et al., 2020). The ozone loss reported in Strahan et al. (2018) for 2015 is similar to the very cold  
175 winters in Antarctica and is slightly higher than that found in our study. The preconditioning for ozone loss in 2013  
176 and 2014 is ensured by the high chlorine activation at the same altitude range (Kuttippurath et al., 2015). Among  
177 the three years prior to the period of the highest ozone loss, the chlorine activation reaches the maximum values in



178 August and September. The chlorine monoxide concentration is found to reach up to 2.2 ppbv in 2013 and 2014,  
179 and 2.0 ppbv in 2015. This high chlorine activation remains for almost a month in the peak ozone loss altitude in  
180 2013 and for lesser duration in 2014 and 2015. The austral springs of 2017 and 2018 also show similar value ranges  
181 for ozone loss, and the chlorine activation in the order of 1.8–2.2 ppbv last for a period of 15–20 days before  
182 attaining the maximum ozone loss.

183 We observe the ozone loss in spring 2016 to be about 3–3.2 ppmv in September and 3.4 ppmv in October. It is also  
184 noticed that the ozone hole, the PSC occurrences, and chlorine activation (more than a month, up to 2.2 ppbv)  
185 lasted longer for the year. An extensive ozone hole is found in 2019 and it lasts from late August to mid-November.  
186 The ozone loss has exceeded up to 3.6 ppmv since late September. However, the ozone concentration enhanced  
187 after the warming and thus the ozone hole size reduced drastically (Fig 3). The chlorine activation is continuous  
188 from August to September (above 2.2 ppbv). The ozone loss values in 2019 and 2020 austral spring are observed  
189 to be much higher than the other years. Despite the episode of minor warming in 2019 (3.0–3.6 ppmv), the ozone  
190 loss was similar to that in 2016. The nature of the spring was similar to previous warm Antarctic years 1988 and  
191 2002. The vortex was short-lived and was highly variable due to increased tropospheric forcing during the year.  
192 The ozone loss in 2019 spring was about 3.6 ppmv, which is higher than 2018 ozone loss during the same period  
193 (Wargan et al., 2020; Roy et al., 2022). The chlorine activation remained at the peak value (2.0–2.2 ppbv) for  
194 several days in August prior to high ozone loss and the spatial distribution (450–550 K) of these high values were  
195 the highest compared to all other years. The 2020 ozone loss was very high (up to 4.6 ppmv) and exceeded the  
196 maximum ozone loss in 2016. The chlorine activation rose remarkably in the early austral spring (September) (2.0–  
197 2.2 ppbv) and is observed to be similar to that in 2016 during this period. Despite the nominal values of chlorine  
198 activation in the 2020 spring, the record values of ozone loss may have resulted from the increased aerosol loading  
199 into the Antarctic atmosphere from the Australian bushfires in 2020 (e.g. Stone et al., 2021).

## 200 201 **Interannual variability of ozone loss for the period 2013–2020.**

202  
203 The interannual variability of ozone loss and chlorine activation are shown in Figure 5. The ozone loss is computed  
204 by taking the mean ozone loss (in ppmv) in the altitude range 450–550 K (the peak ozone loss altitudes) for the day  
205 270 to day 300 day (the peak ozone loss period). Similarly, the chlorine activation (in ppbv) is also estimated as a  
206 mean of the ClO values over the altitude range (450–550 K) for the day 210 to day 270. The weighted mean of





207 PSC area is also shown in the figure in black solid line for the years 2013–2020. It is observed that the lowest ozone  
208 loss is estimated for the years 2015 and 2017 as a result of the minimal chlorine activation prior to the events. The  
209 mean ozone loss is 2.4–2.5 ppmv for both the years and the chlorine activation is about 1.95 ppbv (2015) and 2.15  
210 ppbv (2017). However, the PSC area in 2015 (11.9 million Km<sup>2</sup>) was higher than most of the other cold winters.  
211 Despite the favourable conditions, the low ozone loss was perhaps associated with the relatively weaker chlorine  
212 activation. In the study of Tully et al. (2020), the ozone hole metrics of 2015 is identified to be one of the most  
213 severe and extreme opposed to our results, however, this offset is caused by the difference in the period of  
214 estimation. They have estimated the values of integrated column deficit and ozone hole area metrics for the period  
215 October-December for the corresponding years.

216  
217 The PSC area in 2017 (10.2 million Km<sup>2</sup>) was lower compared to this. The lower value of ozone loss in 2017 spring  
218 is also agreed upon in the analysis conducted by Baarthen (2018). Consistent with the results from the column  
219 ozone loss analysis the highest ozone loss is estimated to be in 2020 (3.8 ppmv) spring followed by 2016 (3 ppmv).  
220 The chlorine activation for both years is also higher than a few other cold winters i.e., 2.2 ppbv in 2016 and 2.3  
221 ppbv in 2020. The high ozone loss in 2020 is favoured by the very large PSC area (12.6 million Km<sup>2</sup>). The 2018  
222 spring was also unique in comparison to the other years of study as a consequence of the high chlorine activation  
223 (2.3 ppbv) and very high PSC area (12.0 million Km<sup>2</sup>). The chlorine activation was the highest in 2019 (2.35 ppbv),  
224 however, the relatively lower ozone loss in the year is observed to be a direct consequence of the unfavourable  
225 dynamic condition (mW). The PSC area is estimated to be the lowest in 2019 (9.4 million Km<sup>2</sup>). The ozone loss in  
226 2013 and 2014 were almost similar (2.7 -2.8 ppmv) and the chlorine activation is in the order of 2.2 and 2.25 ppbv  
227 in 2013 and 2014, respectively.

228  
229

## 230 **CONCLUSION**

231 A major threat that has plagued humanity since its discovery in the early 1980s is the Antarctic ozone hole and its  
232 consequential effects. The ultraviolet (UV) radiation reaching the surface of earth because of the ozone layer  
233 destruction can impact humans and other life forms severely. The effectiveness of Montreal Protocol to control the  
234 emission of these ODSs thus helped in reverting tremendous damage to the life forms on the planet. In addition to  
235 this, ODSs can also cause substantial global warming (Wigley, 1988). Henceforth, a check on their release also  
236 helped in reducing the potential global warming and also on regional climate change. Therefore, the study of





237 interannual ozone variability is important to understand the ozone related changes in the surface climate. Here, we  
238 assess the ozone loss for an 8-year period (2013–2020) in the Antarctic.

239 The year 2019 had a warm winter with a mW in mid-September. The winter 2017 also showed similar  
240 characteristics i.e, there was a sudden increase in temperature during late August, the minimum temperature (about  
241 205 K) was also higher in August than that in other years, and the PSC area showed a sharp decrease towards the  
242 end of September in that year. The heat flux magnitude for the year (2017) was also higher than the other winters  
243 (up to  $-60 \text{ Kms}^{-1}$ ). Conversely, the wave fluxes were the lowest in 2015 winter. The temperature and PSC area  
244 follow similar temporal evolution in 2013, 2014, 2015, 2016 and 2018. The winter 2020 exhibits a unique  
245 meteorology with a long-lasting occurrence of vortex wide PSCs (12.6 million  $\text{Km}^2$ ) and has the highest ozone loss  
246 (3.8-4.0 ppmv). The lowest ozone loss (2.4–2.5 ppmv) was estimated in 2015. We observed a minimal ozone loss  
247 in 2017 and the loss stayed lesser than 2.8 ppmv for most of October and September. Chlorine activation was also  
248 below 1.6–1.8 ppbv in August and September for the year. The study, thus, helps in understanding how the chlorine  
249 activation and meteorology of the years influenced the variability of ozone during the period. It is also observed  
250 that the dynamics and chemistry of the years played their respective roles in the ozone loss process. The winter  
251 2019 is an example of favourable chemistry helping in increased ozone loss though the dynamical conditions were  
252 unfavourable.

### 253 **Acknowledgements**

254 We thank the Indian Institute of Technology Kharagpur, for facilitating the study. We acknowledge free use of the  
255 MLS data, which are taken from <https://disc.gsfc.nasa.gov/>. The meteorological data are acquired through  
256 <https://ozonewatch.gsfc.nasa.gov>. The REPROBUS data are acquired through IPSL, <http://cds-espri.ipsl.fr/>. We  
257 thank Cathy Boone for her help with the model runs, analyses and data transfer, and IPSL for hosting the data.

### 258 **Data availability**

259 The data used in this study are publicly available. The analysed data/codes can also be provided on request.

### 260 **Competing Interests**

261 Jayanarayanan Kuttippurath is a member of the editorial board of Atmospheric Chemistry and Physics.

262



263 **Author Contributions**

264 JK conceived the idea, and JK and RR wrote the original manuscript. The manuscript was subsequently revised  
265 with inputs from PK and FL. The model runs and model results were analyzed by FL. The data analyses and figures  
266 made by RR and PK. All authors participated in discussions and made suggestions, which were considered for the  
267 final draft.

268

269

270

271

272

273

274

275

276

277

278

279

280

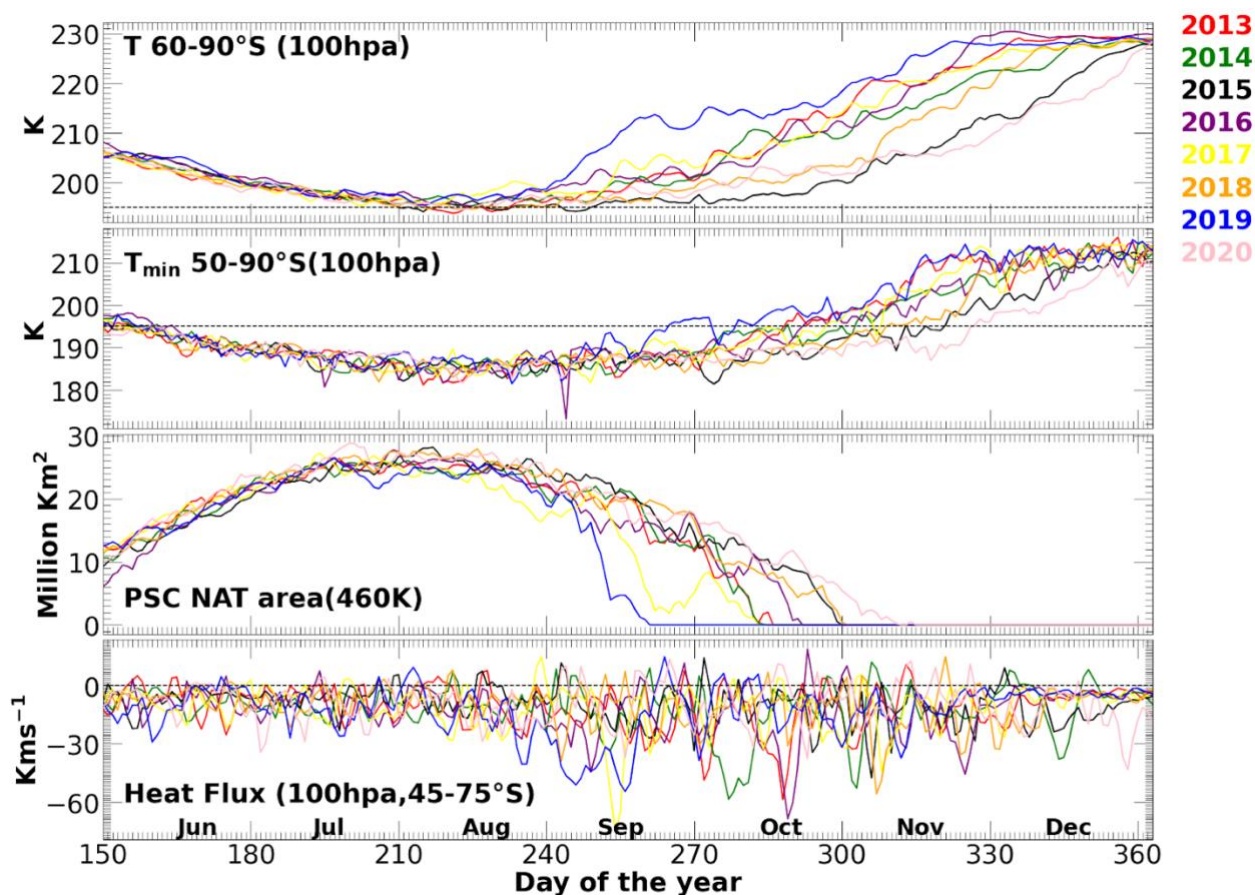
281

282

283

284

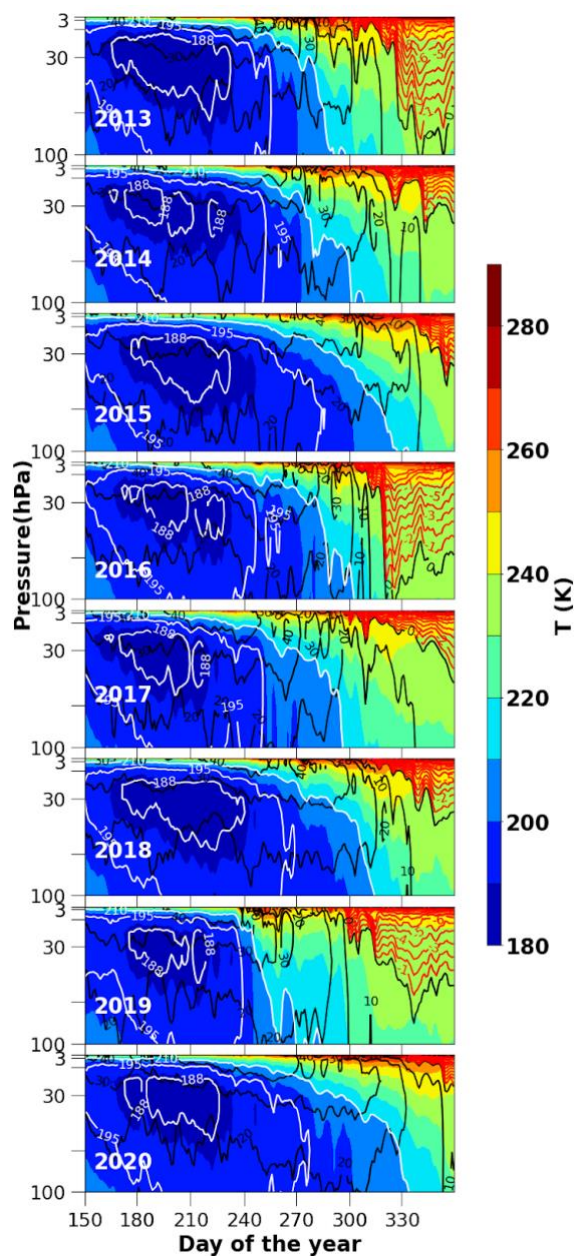
285



286  
287

288 **Figure 1:** Meteorology of the years (2013–2020). First panel shows the zonal average temperature ( $60^{\circ}$ – $90^{\circ}$ S) at  
289 100 hPa. Second panel (from top) shows the minimum temperature at 100 hPa. The black line in the panels show  
290 195 K (PSC formation threshold). Third panel (from top) shows the PSC area at 460 K and the bottom panel shows  
291 the mean heat flux ( $45^{\circ}$ – $75^{\circ}$  S) at 100 hPa. The black horizontal line in the bottom panel shows zero heat flux.

292



293

294

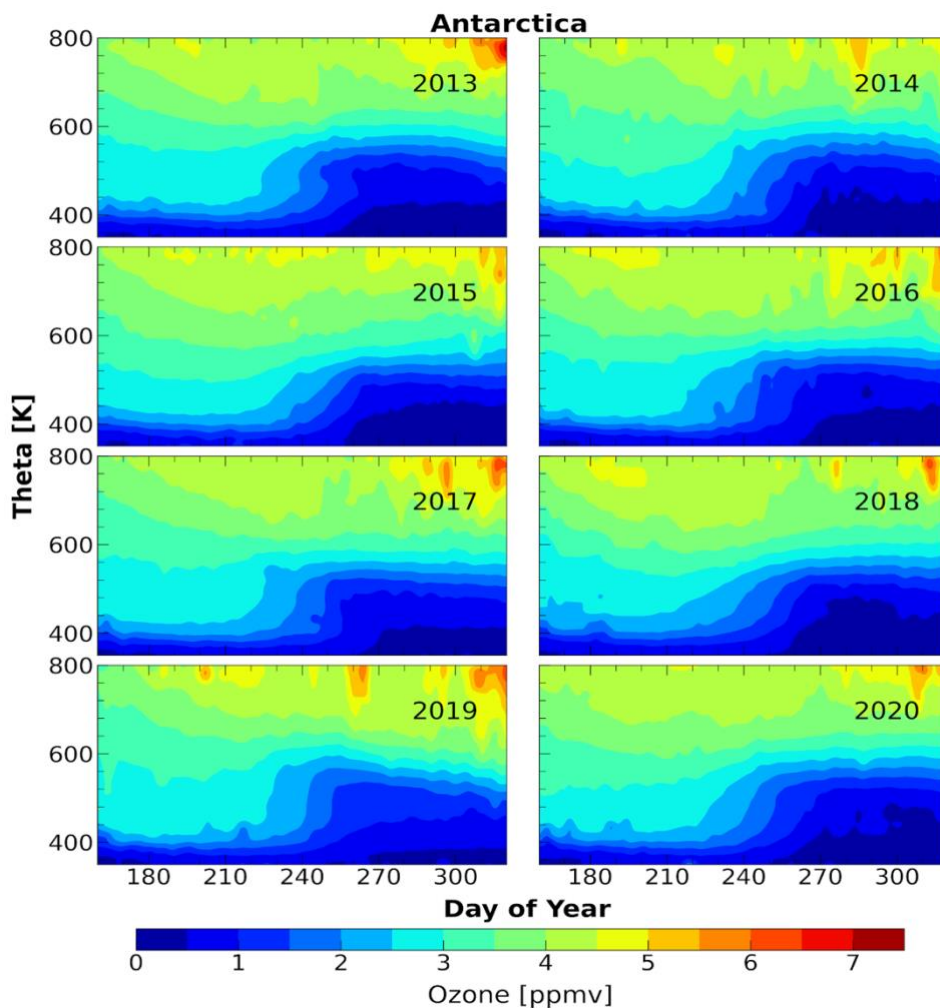
295

296

297

298

**Figure 2:** Seasonal march of the zonal mean temperature for the period 2003–2020 averaged over the latitudes 60–90°S. The contours show the temperature and the white contours represent specific temperatures such as 188, 195 and 210 K. The zonal wind velocities are overlaid. The black contour lines show the westerlies and the red contour lines show the easterlies.

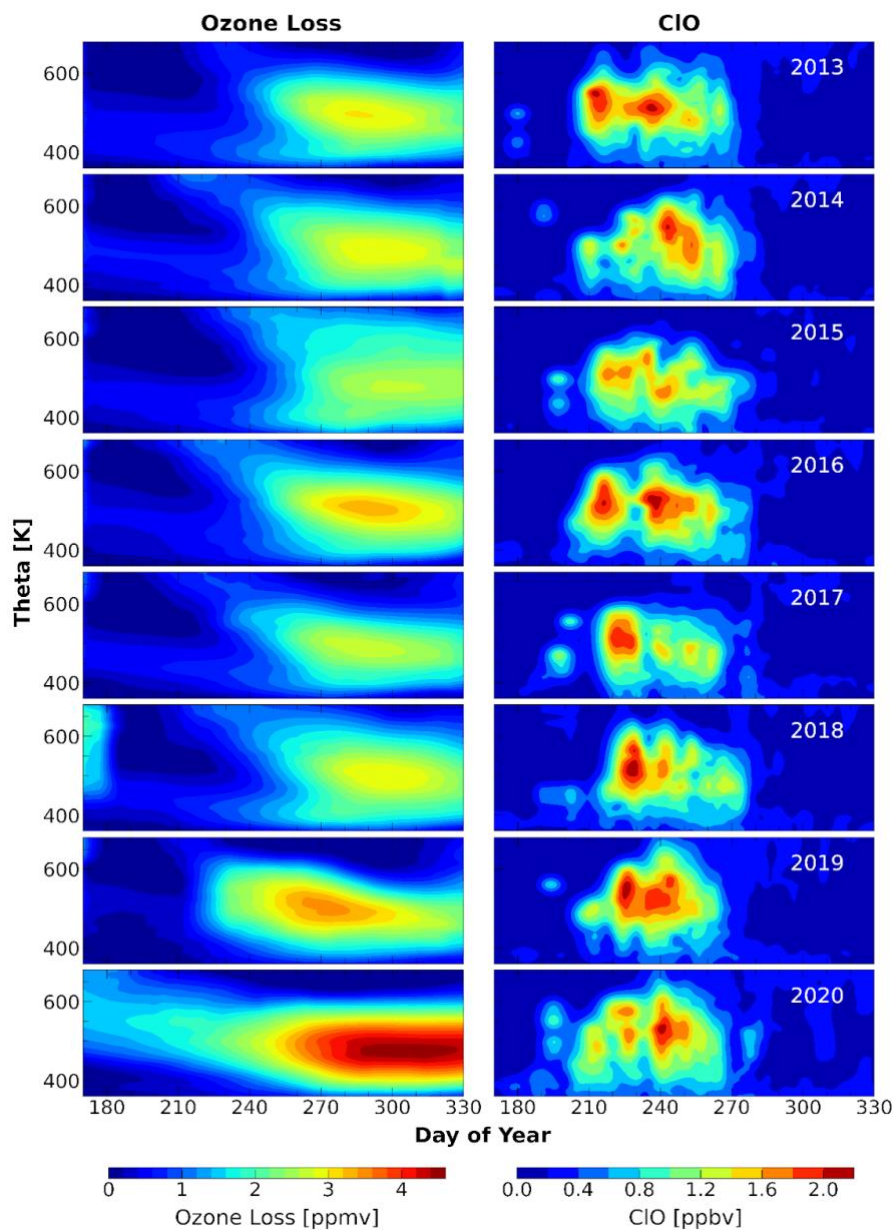


299  
300

301 **Figure 3:** Temporal evolution of the vertical profiles of ozone averaged inside the vortex for the winters from  
302 2013 to 2020 in the Antarctic. MLS data are used for the estimation. The temporal evolution is analysed for the  
303 period June–November and for the altitude range 350–800 K.

304





305

306

307

308

309

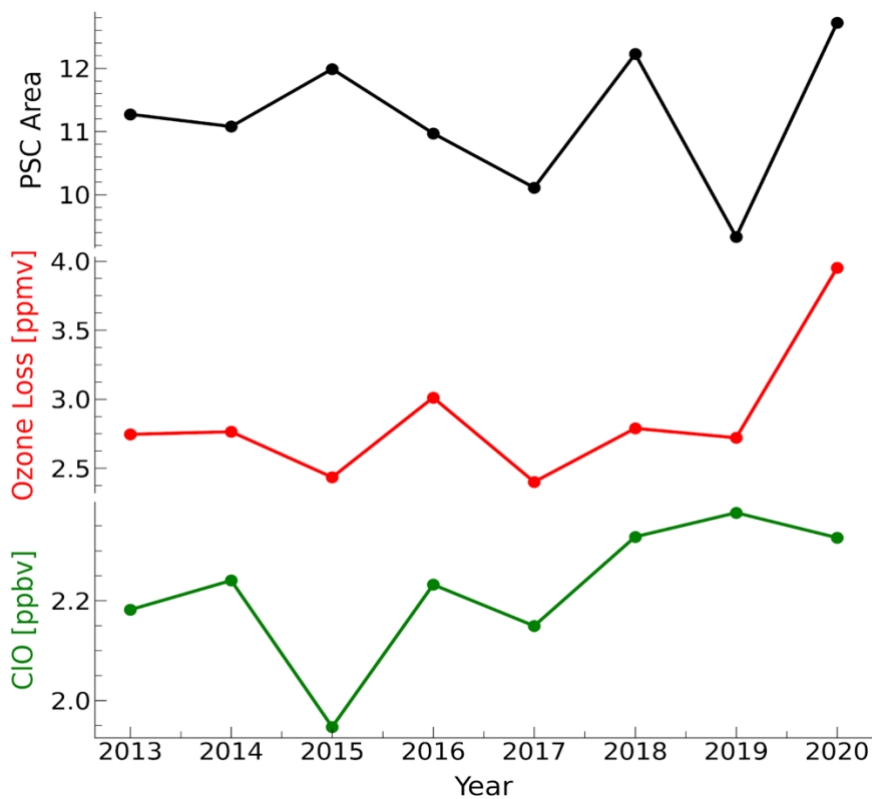
**Figure 4:** Temporal evolution of ozone loss estimated from MLS measurements using REPROBUS passive tracer (left). The MLS CIO measurements for the altitude range 350–700 K for the period 2013–2020. The ozone loss estimates and CIO measurements are selected inside the polar vortex as per the Nash et al. (1996) criterion.



310

311

312



313

314

315 **Figure 5:** The vortex-averaged ozone loss estimated from the MLS measurements using the passive method, peak  
316 ClO measurements, and the weighted average of area of PSC for the period 2013–2020. The mean ozone loss is  
317 estimated over the altitude range 450–550 K for the day 270 and day 300 (maximum ozone loss days). The ClO  
318 measurements are averaged over the altitude range 450–550 K and for the day 210 and day 270; representing the  
319 strong chlorine activation period and altitudes.

320

321

322

323





324 **REFERENCES**

- 325 Angell, J. K. and Free, M.: Ground-based observations of the slowdown in ozone decline and onset of ozone  
326 increase, *J. Geophys. Res.*, 114, D07303, doi:10.1029/2008JD010860, 2009.
- 327 Bandoro, J., Solomon, S., Donohoe, A., Thompson, D.W.J., and Santer, B.D.: Influences of the Antarctic ozone  
328 hole on Southern Hemispheric summer climate change. *Journal of Climate*. 27(16):6245–6264. doi:  
329 10.1175/JCLI-D-13-00698.1, 2014.
- 330 Braathen, G. O.: Observations of the Antarctic Ozone Hole from 2003 to 2017, p. 16503, 2018.
- 331 Butler, A., Daniel, J. S., Portmann, R. W., Ravishankara, A., Young, P. J., Fahey, D. W., and Rosenlof, K. H.:  
332 Diverse policy implications for future ozone and surface UV in a changing climate, *Environ. Res. Lett.*, 11,  
333 064 017, <https://doi.org/10.1088/1748-9326/11/6/064017>, 2016.
- 334 Chipperfield, M. P., Bekki, S., Dhomse, S., Harris, N. R., Hassler, B., Hossaini, R., Steinbrecht, W.,  
335 Thiéblemont, R., and Weber, M.: Detecting recovery of the stratospheric ozone layer, *Nature*, 549, 211,  
336 <https://doi.org/10.1038/nature23681>, 2017.
- 337 Damiani, A., Cordero, R. R., Llanillo, P. J., Feron, S., Boisier, J. P., Garreaud, R., Rondanelli, R., Irie, H., and  
338 Watanabe, S.: Connection between antarctic ozone and climate: Interannual precipitation changes in the Southern  
339 Hemisphere. *Atmosphere*, 11(6), 1–19. <https://doi.org/10.3390/atmos11060579>, 2020.
- 340 de Laat, A. T. J., van Weele, M., and van der A, R. J.: Onset of stratospheric ozone recovery in the Antarctic  
341 ozone hole in assimilated daily total ozone columns, *J. Geophys. Res.-Atmos.*, 122, 11880–11899,  
342 <https://doi.org/10.1002/2016JD025723>, 2017.
- 343 Dee, D. P., Uppala, S. M., Simmons, A. J., Berrisford, P., Poli, P., Kobayashi, S., Andrae, U., Balmaseda, M. A.,  
344 Balsamo, G., Bauer, P., Bechtold, P., Beljaars, A. C. M., van de Berg, L., Bidlot, J., Bormann, N., Delsol, C.,  
345 Dragani, R., Fuentes, M., Geer, A. J., Haimberger, L., Healy S. B., Hersbach, H., Hólm E. V., Isaksen,  
346 L., Kållberg, P., Köhler, M., Matricardi, M., McNally, A. P., Monge-Sanz, B. M., Morcrette J.-J., Park B.-K.,  
347 Peubey, C., de Rosnay, P., Tavolato, C., Thépaut J.-N., and Vitart, F.: The ERA-Interim reanalysis: configuration  
348 and performance of the data assimilation system. *Q. J. R. Meteorol. Soc.*, 137, 553–597.  
349 <https://doi.org/10.1002/qj.828>, 2011.
- 350 Dhomse, S. S., Feng, W., Montzka, S. A., Hossaini, R., Keeble, J., Pyle, J. A., Daniel, J. S., and Chipperfield, M.  
351 P.: Delay in recovery of the Antarctic ozone hole from unexpected CFC-11  
352 emissions. *Nature Communications*, 10(1), 1–12. <https://doi.org/10.1038/s41467-019-13717-x>, 2019.
- 353 Evtushevsky, O. M., Klekociuk, A. R., Kravchenko, V. O., Milinevsky, G. P., and Grytsai, A. V.: The influence  
354 of large amplitude planetary waves on the Antarctic ozone hole of austral spring 2017. *J. South. Hemisph. Earth  
355 Syst. Sci.* 69, 57–64. doi:10.1071/ES19022, 2019.
- 356 Farman, J. C., B. G. Gardiner, and J. D. Shanklin.: Large losses of total ozone in Antarctica reveal seasonal  
357 ClOx/NOx interaction, *Nature*, 315, 207-210, 1985.



- 358 Froidevaux, L., Jiang, Y. B., Lambert, A., Livesey, N. J., Read, W. G.; Waters, J. W., Browell, E. V., Hair, J. W.,  
359 Avery, M. A., McGee, T. J., Twigg, L. W., Sumnicht, G. K., Jucks, K. W., Margitan, J. J., Sen, B., Stachnik, R.  
360 A., Toon, G. C., Bernath, P. F., Boone, C. D., Walker, K. A., Filipiak, M. J., Harwood, R. S., Fuller, R. A.,  
361 Manney, G. L., Schwartz, M. J., Daffer, W. H., Drouin, B. J., Cofield, R. E., Cuddy, D. T., Jarnot, R. F., Knosp,  
362 B. W., Perun, V. S., Snyder, W. V., Stek, P. C., Thurstans, R. P., and Wagner, P. A.: Validation of Aura  
363 Microwave Limb Sounder stratospheric ozone measurements. *Journal of Geophysical Research*, 113(D15),  
364 D15S20–. doi:10.1029/2007jd008771, 2008
- 365 Gelaro, R., McCarty, W., Suárez, M. J., Todling, R., Molod, A., Takacs, L., Randles, C. A., Darmenov, A.,  
366 Bosilovich, M. G., Reichle, R., Wargan, K., Coy, L., Cullather, R., Draper, C., Akella, S., Buchard, V., Conaty,  
367 A., da Silva, A. M., Gu, W., Kim, G.-K., Koster, R., Lucchesi, R., Merkova, D., Nielsen, J. E., Partyka, G.,  
368 Pawson, S., Putman, W., Rienecker, M., Schubert, S. D., Sienkiewicz, M., and Zhao, B.: The Modern-Era  
369 Retrospective Analysis for Research and Applications, Version 2 (MERRA-2), *J. Climate*, 30, 5419–5454,  
370 <https://doi.org/10.1175/JCLI-D-16-0758.1>, 2017.
- 371 Klekociuk, A. R., Tully, M. B., Alexander, S. P., Dargaville, R. J., Deschamps, L. L., Fraser, P. J., Gies, H. P.,  
372 Henderson, S. I., Javorniczky, J., Krummel, P. B., Petelina, S. V., Shanklin, J. D., Siddaway, J. M., and Stone, K.  
373 A.: The Antarctic ozone hole during 2010. *Australian Meteorological and Oceanographic Journal*, 61(4), 253–  
374 267. <https://doi.org/10.22499/2.6104.006>, 2015.
- 375 Krummel, P. B., Fraser, P. J., and Derek, N.: The 2015 Antarctic ozone hole and ozone science summary: final  
376 report. (Report prepared for the Australian Government Department of the Environment, CSIRO:Australia.) iv,  
377 27 pp, 2016.
- 378 Kuttippurath, J., Kumar, P., Nair, P. J., and Pandey, P. C.: Emergence of ozone recovery evidenced by reduction  
379 in the occurrence of Antarctic ozone loss saturation. *Npj Climate and Atmospheric Science*, 1(1).  
380 doi:10.1038/s41612-018-0052-6, 2018.
- 381 Kuttippurath, J., and Nair, P. J.: The signs of Antarctic ozone hole recovery. *Sci. Rep.*, 7, 585,  
382 doi:10.1038/s41598-017-00722-7, 2017.
- 383 Kuttippurath, J., Godin-Beekmann, S., Lefèvre, F., Santee, M. L., Froidevaux, L., and Hauchecorne, A.:  
384 Variability in Antarctic ozone loss in the last decade(2004–2013): high-resolution simulations compared to Aura  
385 MLS observations, *Atmos. Chem. Phys.*, 15, 10385–10397, <https://doi.org/10.5194/acp-15-10385-2015>, 2015.
- 386 Langematz, U., and Kunze, M.: An update on dynamical changes in the Arctic and Antarctic stratospheric polar  
387 vortices. *Clim Dyn* 27, 647–660. <https://doi.org/10.1007/s00382-006-0156-2>, 2006.
- 388 Lefèvre, F., Brasseur, G. P., Folkins, I., Smith, A. K., and Simon, P.: Chemistry of the 1991/1992 stratospheric  
389 winter: three-dimensional model simulation, *J. Geophys. Res.*, 99, 8183–8195, 1994.
- 390 Livesey, N. J., Read, W. G., Froidevaux, L., Lambert, A., Manney, G. L., Pumphrey, H. C., Santee, M. L.,  
391 Schwartz, M. J., Wang, S., Cofield, R. E., Cuddy, D. T., Fuller, R. A., Jarnot, R. F., Jiang, J. H., Knosp, B. W.,  
392 Stek, P. C., Wagner, P. A., and Wu, D. L.: Earth Observing System (EOS) Aura Microwave Limb Sounder  
393 (MLS) Version 3.3 and 3.4 Level 2 data quality and description document, JPL D-33509, Jet Propulsion  
394 Laboratory California Institute of Technology, Pasadena, California, USA, 1–164, 2013.



- 395 Maione, M., Graziosi, F., Arduini, J., Furlani, F., Giostra, U., Blake, D. R., Bonasoni, P., Fang, X., Montzka, S.  
396 A., O'Doherty, S. J., Reimann, S., Stohl, A., and Vollmer, M. K.: Estimates of European emissions of methyl  
397 chloroform using a Bayesian inversion method, *Atmos. Chem. Phys.*, 14, 9755–9770,  
398 <https://doi.org/10.5194/acp-14-9755-2014>, 2014.
- 399 Maliniemi, V., Nesse Tyssøy, H., Smith-Johnsen, C., Arsenovic, P., and Marsh, D.: Ozone super recovery  
400 cancelled in the Antarctic upper stratosphere. *Atmospheric Chemistry and Physics*, February, 1–15.  
401 <https://doi.org/10.5194/acp-2021-149>, 2021
- 402 Milinevsky, G., Evtushevsky, O., Klekociuk, A., Wang, Y., Grytsai, A., Shulga, V., and Ivaniha, O.: Early  
403 indications of anomalous behaviour in the 2019 spring ozone hole over Antarctica. *International Journal of*  
404 *Remote Sensing*, 41(19), 7530–7540. <https://doi.org/10.1080/2150704X.2020.1763497>, 2020.
- 405 Montzka, S. A., G. S. Dutton, P. Yu, E. Ray, R. W. Portmann, J. S. Daniel, L. Kuijpers, B.  
406 D. Hall, D. Mondeel, C. Siso, J. D. Nance, M. Rigby A. J. Manning, L. Hu, F. Moore, B. R. Miller,  
407 and J. W. Elkins.: An unexpected and persistent increase in global emissions of ozone-depleting CFC-11.  
408 *Nature*, 557, 413-417, 2018.
- 409 Müller, R., Tilmes, S., Konopka, P., Groß, J.-U., and Jost, H.-J.: Impact of mixing and chemical change on  
410 ozone-tracer relations in the polar vortex, *Atmos. Chem. Phys.*, 5, 3139–3151, [https://doi.org/10.5194/acp-5-](https://doi.org/10.5194/acp-5-3139-2005)  
411 [3139-2005](https://doi.org/10.5194/acp-5-3139-2005), 2005.
- 412 Nash, E. R., Newman, P. A., Rosenfield, J. E., and Schoeberl, M. R.: An objective determination of the polar  
413 vortex using Ertel's potential vorticity, *J. Geophys. Res.*, 101, 9471–9478, 1996.
- 414 Nedoluha, G. E., Connor, B. J., Mooney, T., Barrett, J. W., Parrish, A., Gomez, R. M., Boyd, I., Allen, D. R.,  
415 Kotkamp, M., Kremser, S., Deshler, T., Newman, P., and Santee, M. L.: 20 years of ClO measurements in the  
416 Antarctic lower stratosphere. *Atmos. Chem. Phys.*, 16(16), 10725–10734. [https://doi.org/10.5194/acp-16-10725-](https://doi.org/10.5194/acp-16-10725-2016)  
417 [2016](https://doi.org/10.5194/acp-16-10725-2016), 2016.
- 418 Pazmiño, A., S. Godin-  
419 Beekmann, A. Hauchecorne, C. Claud, S. Khaykin, F. Goutail, E. Wolfram, J. Salvador, and E. Quel.:  
420 Multiple symptoms of total ozone recovery inside the Antarctic vortex during austral spring. *Atmos. Chem.*  
421 *Phys.*, 18, 7557-7572, 2018.
- 422 Polvani, L. M., Previdi, M., England, M. R., Chiodo, G., and Smith, K. L.: Substantial twentieth-century Arctic  
423 warming caused by ozone-depleting substances. *Nature Climate Change*, 10(2), 130–133.  
424 <https://doi.org/10.1038/s41558-019-0677-4>, 2020.
- 425 Rigby, M., Montzka, S. A., Prinn, R. G., White, J. W. C., Young, D., O'Doherty, S., Lunt, M. F., Ganesan, A. L.,  
426 Manning, A. J., Simmonds, P. G., Salameh, P. K., Harth, C. M., Mühle, J., Weiss, R. F., Fraser, P. J., Steele, L.  
427 P., Krummel, P. B., McCulloch, A., and Park, S.: Role of atmospheric oxidation in recent methane growth.  
428 *Proceedings of the National Academy of Sciences of the United States of America*, 114(21), 5373–5377.  
429 <https://doi.org/10.1073/pnas.1616426114>, 2017



- 430 Rowland, F. S., J. E. Spencer, and M. J. Molina.: Stratospheric formation and photolysis of chlorine nitrate, J.  
431 Phys. Chem., 80, 2711-2713, 1976.
- 432 Roy, R., Kuttippurath, J., Lefèvre, F. et al. The sudden stratospheric warming and chemical ozone loss  
433 in the Antarctic winter 2019: comparison with the winters of 1988 and 2002. *Theor Appl Climatol* 149,  
434 119–130. <https://doi.org/10.1007/s00704-022-04031-6>, 2022
- 435 Salby, M., E. Titova, and L. Deschamps.: Rebound of Antarctic ozone. *Geophys. Res. Lett.*, 38, L09702,  
436 doi:10.1029/2011GL047266, 2011.
- 437 Santee, M., MacKenzie, I. A., Manney, G., Chipperfield, M., Bernath, P. F., Walker, K. A., Boone, C. D.,  
438 Froidevaux, L., Livesey, N., and Waters, J. W.: A study of stratospheric chlorine partitioning based on new  
439 satellite measurements and modeling, *J. Geophys. Res.*, 113, D12307, doi:10.1029/2007JD009057, 2008.
- 440 Shen, X., Wang, L., and Osprey, S.: Tropospheric forcing of the 2019 Antarctic sudden stratospheric warming.  
441 *Geophysical Research Letters*, 47, e2020GL089343. <https://doi.org/10.1029/2020GL089343>, 2020b.
- 442 Shen, X., Wang, L., and Osprey, S.: The Southern Hemisphere sudden stratospheric warming of September 2019.  
443 *Science Bulletin*. doi:10.1016/j.scib.2020.06.028, 2020.
- 444 Solomon, S., Ivy, D. J., Kinnison, D., Mills, M. J., Neely, R. R. III, and Schmidt, A.: Emergence of healing in the  
445 Antarctic ozone layer. *Science*, 252(6296), 269–274. <https://doi.org/10.1126/science.aae006>, 2016.
- 446 Solomon, S.: Stratospheric ozone depletion: A review of concepts and history. *Reviews of Geophysics*, 37(3),  
447 275–316. doi:10.1029/1999rg900008, 1999.
- 448 Solomon, S., Haskins, J., Ivy, D. J., Min, F.: Fundamental differences between Arctic and Antarctic ozone  
449 depletion. *Proceedings of the National Academy of Sciences*, 111(17), 6220–6225.  
450 doi:10.1073/pnas.1319307111, 2014.
- 451 SPARC: Liang, Q., Newman P. A., Reimann, S. (Eds.), Report on the Mystery of Carbon Tetrachloride  
452 (SPARC Report No. 7 WCRP-13/2016) (2016).
- 453 Stolarski, R. S., and R. J. Cicerone.: Stratospheric chlorine: A possible sink for ozone, *Can. J. Chem.*, 52, 1610-  
454 1615, 1974.
- 455 Stolarski, R. S., Douglass, A. R., Gupta, M., Newman, P. A., Pawson, S., Schoeberl, M. R., and Nielsen, J. E.: An  
456 ozone increase in the Antarctic summer stratosphere: A dynamical response to the ozone hole, *Geophys. Res.*  
457 *Lett.*, 33, L21805, doi:10.1029/2006GL026820, 2006.
- 458 Stone, K. A., Solomon, S., Kinnison, D. E., and Mills, M. J.: On recent large Antarctic ozone holes and ozone  
459 recovery metrics. *Geophysical Research Letters*, 48, e2021GL095232. <https://doi.org/10.1029/2021GL095232>,  
460 2021.



- 461 Strahan, S. E., and Douglass, A. R.: Decline in Antarctic ozone depletion and lower stratospheric chlorine  
462 determined from Aura Microwave Limb Sounder observations. *Geophysical Research Letters*, 45, 382– 390.  
463 <https://doi.org/10.1002/2017GL074830>, 2018.
- 464 Strahan, S. E., Douglass, A. R., Newman, P. A., and Steenrod, S. D.: Inorganic chlorine variability in the  
465 Antarctic vortex and implications for ozone recovery. *Journal of Geophysical Research: Atmospheres*, 119,  
466 14,098– 14,109, 2014.
- 467 Tully, M. B., Klekociuk, A. R., Krummel, P. B., Gies, H. P., Alexander, S. P., Fraser, P. J., Henderson, S. I.,  
468 Schofield, R., Shanklin, J. D., and Stone, K. A.: The Antarctic ozone hole during 2015 and 2016. *Journal of*  
469 *Southern Hemisphere Earth Systems Science*, 69(1), 16. <https://doi.org/10.1071/es19021>, 2019.
- 470 Vargin, P.N., Nikiforova, M.P. and Zvyagintsev, A.M.: Variability of the Antarctic Ozone Anomaly in 2011–  
471 2018. *Russ. Meteorol. Hydrol.* 45, 63–73. <https://doi.org/10.3103/S1068373920020016>, 2020.
- 472 Wargan, K., Weir, B., Manney, G. L., Cohn, S. E., and Livesey, N. J.: The anomalous 2019 Antarctic ozone hole  
473 in the GEOS Constituent Data Assimilation System with MLS observations. *Journal of Geophysical Research:*  
474 *Atmospheres*, 125, e2020JD033335. <https://doi.org/10.1029/2020JD033335>, 2020.
- 475 Weatherhead, E. C., Reinsel, G. C., Tiao, G. C., Jackman, C. H., Bishop, L., Hollandsworth Frith, S. M., DeLuisi,  
476 J., Keller, T., Oltmans, S. J., Fleming, E. L., Wuebbles, D. J., Kerr, J. B., Miller, A. J., Herman, J., McPeters, R.,  
477 Nagatani, R. M., and Frederick, J. E.: Detecting the recovery of total column ozone. *Journal of Geophysical*  
478 *Research-Atmospheres*, 105(D17), 22201–22210. <https://doi.org/10.1029/2000JD900063>, 2000.
- 479 Wespes, C., Hurtmans, D., Chabrillat, S., Ronsmans, G., Clerbaux, C., and Coheur, P.-F.: Is the recovery of  
480 stratospheric O<sub>3</sub> speeding up in the Southern Hemisphere? An evaluation from the first IASI decadal record  
481 (2008–2017), *Atmos. Chem. Phys.*, 19, 14031–14056, <https://doi.org/10.5194/acp-19-14031-2019>, 2019.
- 482 Wigley, T.: Future CFC concentrations under the Montreal Protocol and their greenhouse-effect implications.  
483 *Nature* 335, 333–335. <https://doi.org/10.1038/335333a0>, 1988.
- 484 Williamson, D. L. and Rasch, P. J.: Two-dimensional semi-Lagrangian transport with shape-preserving  
485 interpolation, *Mon. Weather Rev.*, 117, 102–129, 1989.
- 486 WMO (World Meteorological Organization): Scientific Assessment of Ozone Depletion: 2006, Global Ozone  
487 Research and Monitoring Project – Report No. 50, 572 pp., Geneva, 2007
- 488 WMO: Scientific Assessment of Ozone Depletion: 2014 Global Ozone Research and Monitoring Project Report,  
489 World Meteorological Organization, Geneva, Switzerland, p. 416, 2014.
- 490 World Meteorological Organization (WMO) (2015), WMO Antarctic Ozone Bulletins (2015). [Available at  
491 [www.wmo.int/pages/prog/arep/WMOAntarcticOzoneBulletins2015.html](http://www.wmo.int/pages/prog/arep/WMOAntarcticOzoneBulletins2015.html).]
- 492 Yamazaki, Y., Matthias, V., Miyoshi, Y., Stolle, C., Siddiqui, T., Kervalishvili, G., LaÅ;toiviÄka, J., Kozubek,  
493 M., Ward, W., Themens, D. R., Kristoffersen, S., Alken, P.: September 2019 Antarctic Sudden Stratospheric



- 494 Warming: Quasi-Daily Wave Burst and Ionospheric Effects. *Geophysical Research Letters*, 47(1), –.  
495 doi:10.1029/2019GL086577, 2020.
- 496 Yang, E.-S., Cunnold, D. M., Newchurch, M. J., Salawitch, R. J., McCormick, M. P., Russell, J. M., Zawodny, J.  
497 M., and Oltmans, S. J.: First stage of Antarctic ozone recovery, *J. Geophys. Res.*, 113, D20308,  
498 <https://doi.org/10.1029/2007JD009675>, 2008.
- 499 Zhang, Y., Li, J., and Zhou, L.: The Relationship between Polar Vortex and Ozone Depletion in the Antarctic  
500 Stratosphere during the Period 1979–2016. *Advances in Meteorology*, 2017, 1–12. doi:10.1155/2017/3078079,  
501 2017.
- 502 Zuev, V. V., and Savelieva, E.: The cause of the spring strengthening of the Antarctic polar vortex. *Dynamics of*  
503 *Atmospheres and Oceans*, 87, 101097. doi:10.1016/j.dynatmoce.2019.101097, 2019.
- 504
- 505
- 506
- 507
- 508
- 509 V08/JK/04112021
- 510
- 511